This article has been accepted for publication in a future issue of this journal, but has not been fully edited. Content may change prior to final publication. Citation information: DOI 10.1109/TSTE.2016.2546279, IEEE Transactions on Sustainable Energy

Impacts of Stochastic Wind Power and Storage Participation on Economic Dispatch in Distribution Systems

Abebe W. Bizuayehu, *Member, IEEE,* Agustín A. Sánchez de la Nieta, *Member, IEEE*
Javier Contreras, *Fellow, IEEE*, and João P. S. Catalão, *Senior Member, IEEE*

***Abstract*—Evaluating the impact related to stochastic wind generation and generic storage on economic dispatch in distribution system operation is an important issue in power systems. This paper presents the analysis of the impacts of high wind power and storage participation on a distribution system over a period of 24 hours using grid reconfiguration for Electrical Distribution System (EDS) radial operation. In order to meet this objective, a stochastic mixed integer linear programming (SMILP) is proposed, where the balance between load and generation has to be satisfied minimizing the expected cost during the operation period. The model also considers distributed generation (DG) represented by wind scenarios and conventional generation, bus loads represented through a typical demand profile, and generic storage. A case study provides results for a weakly meshed distribution network with 70 buses, describing in a comprehensive manner the effects of stochastic wind scenarios and storage location on distribution network parameters, voltage, substation behavior as well as power losses and the expected cost of the system.**

***Index Terms*—Distributed generation, distribution system reconfiguration (DSR), generic storage, stochastic mixed integer linear programming (SMILP), wind generation.**

NOMENCLATURE

Indexes

i, j, k	Indexes referring to a bus.
f	Index for the f^{th} partition segment of the blocks used for the linearization (f=1, 2,..., F).
t	Index referring to a period [hour].
w	Index referring to a scenario.
m	Number of branches of the EDS.

Parameters

C^C	Costs of conventional generators [€/kWh].
C^{LOSS}	Costs of resistive losses [€/kWh].
C^{NS}	Costs of unserved energy [€/kWh].
C^{RN}	Costs of wind power [€/kWh].
C^{St}	Costs of the generic storage [€/kWh].
C^S	Costs of energy from the substation [€/kWh].
E^{St}_{max}	Maximum energy storage capacity [kWh].
F	Number of blocks used for the linearization.
$I^{MAX}_{i,j}$	Maximum current flow through branch *ij* [A].
N	Number of buses.
$P^D_{i,t}$	Active power demand at bus *i* and period *t* [kW].
$P^{RN}_{i,t,w}$	Active wind power generation at bus *i*, period *t* and scenario *w* [kW].
P^{SC}_{max}	Maximum storage charging power [kW].
P^{SD}_{max}	Maximum storage discharging power [kW].
$Q^D_{i,t}$	Reactive demand at bus *i* and period *t* [kVAr].
$R_{i,j}$	Resistance of branch *ij* [Ω].
$\Delta S_{i,j,f,t,w}$	Upper limits for the discretization of the apparent power through branch *ij* [kVA].
ρ_w	Probability of each scenario *w*.
U^{MAX}	Upper limits of voltage drop in switches [V].
V^{NOM}	Nominal voltage of the network [V].
$V2^{NOM}_{i,t,w}$	Quadratic nominal voltage of the network at bus *i*, period *t* and scenario *w* [V^2].
$X_{i,j}$	Reactance of branch *ij* [Ω].
$Z_{i,j}$	Impedance of branch *ij* [Ω].
η_c	Storage charging efficiency.
η_d	Storage discharging efficiency.

Continuous Variables

$Cost$	Expected costs [€].
$E^{St}_{i,t}$	Energy stored at bus *i*, period *t* [kWh].
$I2_{i,j,t,w}$	Square of the current flow of branch *ij* at period *t* and scenario *w* [A^2].
$P^C_{i,t}$	Active power of the conventional generation at bus *i* and period *t* [kW].
$P^S_{i,t}$	Active power of the substation at bus *i* and period *t* [kW].
$P^{SC}_{i,t}$	Storage charging power at bus *i* and period *t* [kW].
$P^{SD}_{i,t}$	Storage discharging power at bus *i* and period *t* [kW].
$P^{NS}_{i,t}$	Unserved power at bus *i* and period *t* [kW].
$P^{+}_{i,j,t,w}$	Downstream active power of branch *ij* in period *t* and scenario *w* [kW].
$P^{-}_{i,j,t,w}$	Upstream active power of branch *ij* in period *t* and scenario *w* [kW].
$Q^C_{i,t}$	Reactive power of conventional generation at bus *i* and period *t* [kVAr].
$Q^{RN}_{i,t,w}$	Renewable reactive power at bus *i*, period *t* and scenario *w* [kVAr].

This work was supported by FEDER funds (European Union) through COMPETE and by Portuguese funds through FCT, under Projects FCOMP-01-0124-FEDER-020282 (Ref. PTDC/EEA-EEL/118519/2010) and UID/CEC/50021/2013. Also, the research leading to these results has recieved funding from the EU Seventh Framework Programme FP7/2007-2013 under grant agreement no. 309048.

Abebe W. Bizuayehu, Agustín A. Sánchez de la Nieta and João P. S. Catalão are with the Faculty of Engineering of the University of Porto, Porto, with the University of Beira Interior (UBI), Covilhã, and with INESC-ID, Inst. Super. Tecn., University of Lisbon, Portugal (e-mail: buzeabebe@gmail.com; agustinsnl@gmail.com; catalao@ubi.pt).

Javier Contreras is with E.T.S. de Ingenieros Industriales, Universidad de Castilla-La Mancha, 13071 Ciudad Real, Spain (e-mail: Javier.Contreras@uclm.es).

This article has been accepted for publication in a future issue of this journal, but has not been fully edited. Content may change prior to final publication. Citation information: DOI 10.1109/TSTE.2016.2546279, IEEE Transactions on Sustainable Energy

$Q^{S}_{i,t}$	Reactive power of the substation at bus *i* and period *t* [kVAr].
$Q^{+}_{i,j,t,w}$	Downstream reactive power of branch *ij* in period *t* and scenario *w* [kVAr].
$Q^{-}_{i,j,t,w}$	Upstream reactive power of branch *ij* in period *t* and scenario *w* [kVAr].
$V2_{i,t,w}$	Square of voltage at bus *i*, period *t* and scenario *w* [V^2].
$U_{i,j,t,w}$	Auxiliary variable for voltage drop in branch *ij*, period *t* and scenario *w* in case the switch is open [V].
$\Delta P_{i,j,f,t,w}$	Value of active power in branch *ij* of block *f*, period *t* and scenario *w* [kW].
$\Delta Q_{i,j,f,t,w}$	Value of reactive power in branch *ij* of block *f*, period *t* and scenario *w* [kVAr].

Binary Variables

α_l	Binary variable for branch status in each period; 0 when branch *ij* is open, and 1 otherwise.
$B_{i,j}$	Binary variable set to 1, if node *j* is the parent of node *i*, and 0 otherwise.
$N^{St}_{i,t}$	Binary variable set to 1, if storage is charging at bus *i*, period *t* and 0 otherwise.

I. Introduction

The improvement of the operational behavior of distribution systems under high wind penetration and the participation of storage systems is one of the current challenges in the power system industry. With the current advances in smart grids, the evaluation of the operational behavior, in addition to the quality of the power delivery, stability and minimization of grid operation costs, should consider environmental impact issues as well as the benefits of the stakeholders.

A. Literature review

Distribution systems represent the final link between the bulk power supply system and the consumers, therefore, in order to understand their behavior in the presence of DG, it is crucial to have accurate operation analysis tools [1]. In addition, a significant amount of power loss is attributed to line losses in distribution systems, estimated according to [2] around 10-13%. The most common method used in EDS for voltage enhancement and the minimization of power losses is the integration of DG and capacitor placement. There are other practices to improve distribution system operation, which has been explored in [3] – [9], where other methods handle the economic dispatch problem, like the use of network reconfiguration and the optimal placement of storage. The optimal placement of DG helps to improve the utilization of the maximum possible amount of available resources, rather than responding to the dispatch instructions of the grid operator [6]. However, these improvement possibilities are blurred by the complex factors involved in the technical and decision aspects of grid operation. Moreover, DG power integration in EDS must satisfy certain requirements like voltage stability, current limits and reactive power requirements, which are of great relevance for the EDS secured operation [2].

Another important issue is the integration of intermittent energy resources, specifically wind. Due to their high volatility, it is difficult to guarantee a continuous power supply from this kind of generation source. In addition, this situation is exacerbated in the case of higher wind penetration levels due to their non-dispachable nature and variability, resulting in a significant operational challenge in distribution systems [10]. Therefore, the integration of intermittent distributed energy sources for the satisfaction of a flexible demand scheme involves a need for advanced decision making tools, as well as additional operational flexibility to guarantee grid stability and economic operation [11] – [13]. The study presented in [13] proposes a model with energy storage to investigate the economic advantage of wind and storage co-location at different buses, indicating that the integration of intermittent energy resources with higher level of penetrations should be supported using increased operational flexibility. The suggestion indicates that such support in flexibility can be achieved using energy storage systems, even though their impact depends on the type and the level of penetration of renewable generation.

Concerning solution approaches, several mixed integer linear models have been used in literature to minimize operation costs, considering load and wind power production as stochastic inputs [5]. The solution method based on a stochastic approach has a series of benefits compared to a deterministic approach, because the stochastic approach allows us to accommodate a higher wind power penetration level without sacrificing power security [6]. In relation to the commercial maturity of the solvers, MILP solvers have greater advantage over solvers for MINLP; in addition, MILP solvers facilitate an easier formulation and a flexible approach for discrete decision making, as suggested by [14].

B. Aims and contributions

The main goal of this paper is to evaluate the operational performance of EDS connected to the main power grid through a substation, in the presence of DG, considering the impacts of stochastic wind generation, generic storage systems; minimizing the cost of active power losses, the cost of generations for each technology and the unserved energy. The novelty of this work is the analysis of the simultaneous impacts of wind participation and grid reconfiguration on economic dispatch on a daily and hourly basis, as well as the impact of storage location on the minimization of the expected EDS operational costs. In addition, we aim to illustrate the validity of a linearized model to evaluate the joint interaction and impact of high wind power participation, generic storage systems and conventional generation on economic dispatch problems. The main contributions of this work are:

1) A SMILP model is used to evaluate the joint impact of stochastic wind power and a generic storage system participation on economic dispatch.
2) A linearized model including EDS reconfiguration with optimum radial topology to increase wind power participation is shown.
3) A sensitivity analysis and evaluation of the optimal economic dispatch is conducted for different storage costs and storage relocations.

This article has been accepted for publication in a future issue of this journal, but has not been fully edited. Content may change prior to final publication. Citation information: DOI 10.1109/TSTE.2016.2546279, IEEE Transactions on Sustainable Energy

The paper is structured in the following way: Section II provides the description of the problem related to EDS analysis, Section III describes the mathematical formulation of the problem, Section IV presents the case study, Section V presents the main results obtained and relevant conclusions are drawn in Section VI.

II. Description of the Problem

Evaluating the impact of the aforementioned multiple factors on EDS behavior is a complex task. In addition, this type of challenging distribution operation analysis involves discrete decisions to guarantee the optimum solution to improve voltage profile, to meet demand and, at the same time, to manage system imbalances. The integration of wind resources into EDS network changes the expected behavior of the network, the power injection being real or reactive depending on system demand and wind power availability at the point of connection. Hence, this has a significant impact on the operation of low voltage networks, and, even in extreme cases, extended impacts occur in the upstream medium voltage network. Therefore, a grid operating under such circumstances requires increasing operational flexibility and timely decisions, and some of the alternative solutions to guarantee such flexibility are the use of storage systems and grid reconfiguration.

In order to evaluate the degree of the impacts of these random variations on wind power generation and storage participation (on an hourly basis and throughout the day) in low voltage distribution systems, the behavior of the EDS needs to be studied so that any unexpected operational behavior of the network arising from wind integration can be addressed. In the present model a SMILP approach is proposed to analyze the optimum operation of a 70-bus EDS, shown in Fig. 1, minimizing operational cost and losses. Hence, the distribution network behavior is studied in a comprehensive manner under high wind power scenarios, with storage participation to stabilize power fluctuations and the uncertainties introduced by wind generation.

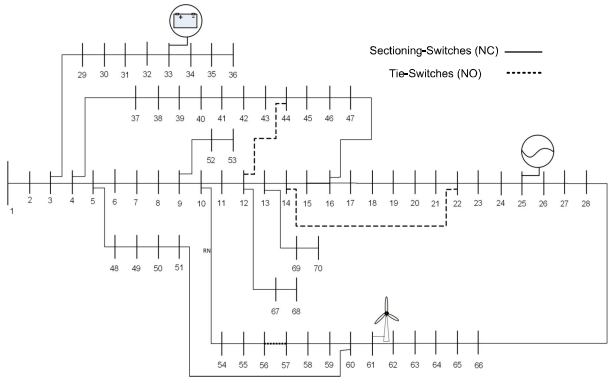

Fig. 1. 70-bus distribution system.

The theoretical power flow analysis for the current model is based on the premise of a basic EDS operation, where the model is applied to evaluate the performance of a weakly meshed distribution grid.

For the problem formulation, the following assumptions are taken into consideration [15]:

1) The EDS is assumed to be balanced and represented by its single-phase equivalent model.
2) In branch *ij*, bus *i* is closer to the substation than bus *j*.
3) Active and reactive power losses in branch *ij* are concentrated at bus *j*.
4) Switches exist in all the branches of the network.

Despite the above assumptions, two kind of switches, tie-switches and sectionalizing switches, are identified in this model. The optimal configuration is achieved using a mathematical formulation of the problem. In order to handle the status of sectionalizing switches (normally closed) and tie switches (normally open) the algorithm uses binary variables, so that the radiality of the network is maintained and all the loads are supplied. There are no special built-in reconfiguration switching sequences, however, the mathematical formulation pursues to establish the optimum flow pattern and the radiality in the network.

III. Problem Formulation

The formulation consists of two parts: objective function and constraints.

A. Objective function

The objective is to minimize the expected operational cost of losses, the cost of generations for each technology and the cost of the unserved energy in the distribution network with wind generation and storage participation as expressed in (1). It is important to note that, in (1), the term I2 is the squared current, I^2, playing the role of a linear expression for the branch *ij* squared current. In order to reverse the situation once the optimization process is finalized, the current through branch *ij* is computed solving the square root of the I2 output.

$$\begin{aligned}\min \quad Cost = \sum_{w} \rho_w \sum_{t} \sum_{i,j} \Big(& R_{i,j} \cdot I2_{i,j,t,w} \cdot C^{LOSS} \\ & + P^{RN}_{i,t,w} \cdot C^{RN} + P^{C}_{i,t} \cdot C^{C} + P^{S}_{i,t} \cdot C^{S} \\ & + P^{SC}_{i,t} \cdot C^{St} + P^{SD}_{i,t} \cdot C^{St} + P^{NS}_{i,t} \cdot C^{NS} \Big) \end{aligned} \tag{1}$$

The operational marginal cost components of the equation are wind power marginal cost, conventional power marginal cost, substation or grid power marginal cost, storage charging and discharging power marginal cost and unserved power marginal cost. The continuous variable for unserved power is a marginal cost component of the objective function considered to penalize (assigning higher costs) the power not supplied in case the power demand is not satisfied at the specific bus.

B. Constraints

The block of constraints is presented as follows.

1) Power balance constraints: The expressions for the active and reactive power balances for the network are presented in (2) and (3), where the demand should be met by the generation at each bus. Since the integration of DG introduces a reverse power flow pattern on EDS branches, a convention to accommodate both flow directions in branches is adopted [16], [17] and [18]. Hence, the net flow in branches is considered as the difference between the normal flow (downstream) and

This article has been accepted for publication in a future issue of this journal, but has not been fully edited. Content may change prior to final publication. Citation information: DOI 10.1109/TSTE.2016.2546279, IEEE Transactions on Sustainable Energy

the reverse flow (upstream). This convention is applied to the power balance equation, where the generation power, the net power flow and the line power loss terms are considered on the left hand of the equation, and the power demand, the storage charge and discharge power as well as the unserved power are considered on the right hand side of the equation, for each scenario and period as presented below:

$$\begin{aligned} &P^{S}_{i,t} + P^{C}_{i,t} + P^{RN}_{i,t,w} \\ &- \sum_{j}[(P^{+}_{i,j,t,w} - P^{-}_{i,j,t,w}) + R_{i,j} \cdot I2_{i,j,t,w}] \\ &+ \sum_{j}(P^{+}_{j,i,t,w} - P^{-}_{j,i,t,w}) = P^{D}_{i,t} + P^{SC}_{i,t} - P^{SD}_{i,t} - P^{NS}_{i,t}; \end{aligned} \tag{2}$$

$$\begin{aligned} &Q^{S}_{i,t} + Q^{C}_{i,t} + Q^{RN}_{i,t,w} \\ &- \sum_{j}[(Q^{+}_{i,j,t,w} - Q^{-}_{i,j,t,w}) + X_{i,j} \cdot I2_{i,j,t,w}] \\ &+ \sum_{j}(Q^{+}_{j,i,t,w} - Q^{-}_{j,i,t,w}) = Q^{D}_{i,t}. \end{aligned} \tag{3}$$

In the optimization objective function we are minimizing power losses, among other terms, given by $R\ I^2$, where $I^2 \approx ((P^2 + Q^2)/V^2)$. Moreover, bus voltage angles are assumed to be close to zero, and bus voltage magnitude differences are negligible, leading to $V \approx V_{nominal}$ and, therefore, to $I^2 \approx ((P^2 + Q^2)/(V_{nom})^2)$. This expression is the same as equation (10) of the paper, i.e. $V^2_{nom} I^2 \approx P^2 + Q^2$, where the quadratic active and reactive power flows are linearized in a piecewise fashion according to the expressions in (11)-(15), avoiding the quadratic terms. This piecewise linearization method has been proved to be very effective, with a maximum approximation error of 0.34%, according to [17]. Hence, the active and reactive power limits are expressed separately, as in (11) and (12) to facilitate the linearization. Therefore, the constraints for the maximum branch capacities are expresed in (4) for active and in (5) for reactive power:

$$0 \leq (P^{+}_{i,j,t,w} + P^{-}_{i,j,t,w}) \leq V^{NOM} \cdot I^{MAX}_{i,j}; \tag{4}$$

$$0 \leq (Q^{+}_{i,j,t,w} + Q^{-}_{i,j,t,w}) \leq V^{NOM} \cdot I^{MAX}_{i,j}. \tag{5}$$

2) Nominal voltage balance constraints: The nominal voltage balance equation for the whole network is provided in equation (6) considering line voltage drops in *ij* branches and an auxiliary variable, $U_{i,j,t,w}$, that accounts for the voltage drop to satisfy the voltage balance during switching operations. These auxiliary variables are also considered for the voltage drop limits given in equations (7) and (8).

$$\begin{aligned} &V2_{i,t,w} - V2_{j,t,w} + U_{i,j,t,w} - 2 \cdot [R_{i,j} \cdot (P^{+}_{i,j,t,w} - P^{-}_{i,j,t,w}) \\ &+ X_{i,j} \cdot (Q^{+}_{i,j,t,w} - Q^{-}_{i,j,t,w})] - Z^2_{i,j} \cdot I2_{i,j,t,w} = 0. \end{aligned} \tag{6}$$

Constraints in (7) and (8) represent the auxiliary variables corresponding to the upper and lower limits of permissible voltage drops in switches during maneuvers. Furthermore, the maximum current limits for each branch are presented in (9):

$$U_{i,j,t,w} \leq U^{MAX}(1 - \alpha_l); \tag{7}$$

$$U_{i,j,t,w} \geq -U^{MAX}(1 - \alpha_l); \tag{8}$$

$$0 \leq I2_{i,j,t,w} \leq (I^{MAX}_{i,j})^2 \cdot \alpha_l. \tag{9}$$

3) Power linearization constraints: Equation (10) relates the product of quadratic voltages and currents with the finite sum of the linearized terms of the corresponding set of piecewise linear equations.

$$\begin{aligned} V2^{NOM}_{i,t,w} \cdot I2_{i,j,t,w} &= \sum_{f}((2f-1)\Delta S_{i,j,f,t,w} \cdot \Delta P_{i,j,f,t,w}) \\ &+ \sum_{f}((2f-1)\Delta S_{i,j,f,t,w} \cdot \Delta Q_{i,j,f,t,w}. \end{aligned} \tag{10}$$

The linearization of the non-linear terms is carried out using a set of linear equations from (11)–(15). These equations constitute the core expressions for the proposed stochastic mixed integer linear model where the non-linear terms are linearized. Detailed descriptions and further justifications about the linearization process are found in [15] and [19]. The piecewise linearization for the active and reactive approximations are:

$$(P^{+}_{i,j,t,w} + P^{-}_{i,j,t,w}) = \sum_{f} \Delta P_{i,j,f,t,w}; \tag{11}$$

$$(Q^{+}_{i,j,t,w} + Q^{-}_{i,j,t,w}) = \sum_{f} \Delta Q_{i,j,f,t,w}; \tag{12}$$

$$0 \leq \Delta P_{i,j,f,t,w} \leq \Delta S_{i,j,f,t,w}; \tag{13}$$

$$0 \leq \Delta Q_{i,j,f,t,w} \leq \Delta S_{i,j,f,t,w}; \tag{14}$$

$$\Delta S_{i,j,f,t,w} = \frac{V^{NOM} \cdot I^{MAX}_{i,j}}{F}. \tag{15}$$

4) Radiality constraints: Constraint (16) is a necessary condition to maintain radiality. However, this condition is necessary but not sufficient, as shown in [4], [16], [20] and [17]. In order to reinforce the radiality constraints, some authors suggest a loop approach [21], [22] and others a spanning tree [14], [17] searching for a single parent as a necessary condition to have a radial network topology as described in [19], [23] and [24].

However, in the present case, this limitation can be overcome by enforcing local loop radiality constraints in order to limit the number of branches opened at a time in the spanning tree. Equation (16) indicates that branch *ij* is in the spanning tree (α_l=1), either if node *j* is the parent of node *i* ($B_{i,j}$=1) or node *i* is the parent of node *j* ($B_{j,i}$=1). Equation (18) requires every node excluding the substation node to have exactly one parent, while (19) indicates that the substation node has no parents.

$$\sum_{l=1}^{m} \alpha_l = N - 1; \tag{16}$$

$$B_{i,j} + B_{j,i} = \alpha_l; \tag{17}$$

$$\sum_{j \in N_i} B_{i,j} = 1, i = 2, ..., n; \tag{18}$$

$$B_{1,j} = 0; \tag{19}$$

This article has been accepted for publication in a future issue of this journal, but has not been fully edited. Content may change prior to final publication. Citation information: DOI 10.1109/TSTE.2016.2546279, IEEE Transactions on Sustainable Energy

$$B_{i,j} \in \{0,1\}; \tag{20}$$

$$0 \leq \alpha_l \leq 1. \tag{21}$$

In the proposed model, all branches either have interconnections or sectionalizing switches, which can be opened or closed using binary variable $B_{j,i}$ in order to respect the branch capacity limits according to (17), until the best topology is found. In the formulation presented $B_{j,i,t}$ is used to account for the hourly reconfiguration analysis.

5) Power factor constraints: Equations (22)–(25) are constraints relating active and reactive power for renewable and conventional generation to account for positive and negative rates of the power factor, respectively. The power factor constraints for wind power are shown in (22) and (23), while (24) and (25) are the rates of the power factors for conventional generators:

$$Q^{RN}_{i,t,w} \leq P^{RN}_{i,t,w} \cdot \tan(\arccos(0.95)); \tag{22}$$

$$Q^{RN}_{i,t,w} \geq P^{RN}_{i,t,w} \cdot \tan(\arccos(\text{-}0.95)); \tag{23}$$

$$Q^{C}_{i,t} \leq P^{C}_{i,t} \cdot \ \tan(\arccos(0.95)); \tag{24}$$

$$Q^{C}_{i,t} \geq P^{C}_{i,t} \cdot \tan(\arccos(\text{-}0.95)). \tag{25}$$

6) Generic storage constraints: Equations (26)-(30) are constraints relating storage power and energy [25] and [26]. The storage transition function (26), storage limits (27), storage initialization (28), the initial state of the storage is assumed to be 50% of its storage capacity, storage withdrawal from the network (29) and storage injection into the network (30) are given by:

$$E^{St}_{i,t} = E^{St}_{i,t-1} + P^{SC}_{i,t} \cdot \eta_c - \frac{P^{SD}_{i,t}}{\eta_d}; \tag{26}$$

$$0 \leq E^{St}_{i,t} \leq E^{St}_{max}; \tag{27}$$

$$E^{St}_{i,t=0} \leq \frac{E^{St}_{max}}{2}; \tag{28}$$

$$0 \leq P^{SC}_{i,t} \leq P^{SC}_{max} \cdot N^{St}_{i,t}; \tag{29}$$

$$0 \leq P^{SD}_{i,t} \leq P^{SD}_{max} \cdot (1 - N^{St}_{i,t}). \tag{30}$$

IV. Case Study

A. Case study network

A case study for the analysis of the operation is carried out in the 70-bus EDS network shown in Fig. 1. As illustrated by the figure, the EDS is connected to a substation at node 1, conventional generation is located at node 25 with a maximum capacity of 0.3 p.u., wind generation is located at node 61 with a maximum capacity of 1.71 MVA, which represents a penetration level of 36.6%, and a storage unit is connected at node 33 with a maximum capacity of 0.3 p.u. The number of blocks used for the linearization is 5. A higher number of blocks would be more CPU-time consuming but the results obtained were practically the same. In order to evaluate the degree of impacts of wind participation and storage on the economic dispatch of the distribution system, two types of operation setups are considered. The first setup is the base case with an active power of 3.802 kW and a reactive power of 2.694 kVAr, where no participation of distributed resources is taking place, this being our benchmark distribution system for operation analysis. Hence, the total power demand in the distribution network is met using a single substation connected to the grid, while, for the second setting, the substation together with the grid are connected to distributed resources comprising conventional generation, wind generation and storage. In addition, the EDS has two types of reconfigurations: i) the daily configuration, which is a fixed configuration during a period of 24 hours, with the possibility to curtail part of the wind production, and ii) the hourly configuration, where the EDS is reconfigured every hour, allowing to absorb the entire wind production.

In both cases, the aim is to satisfy a maximum peak load of 4.66 MVA during a period of 24 hours. The economic impact of wind generation as well as the storage participation is evaluated through sensitivity analysis. An additional impact assessment is made swapping the storage location with conventional generation, the initial storage location being at node 33 and conventional generation at node 25, as illustrated in Fig. 1.

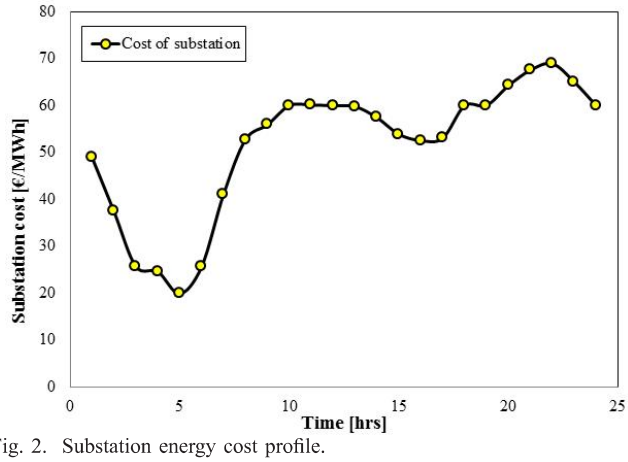

Fig. 2. Substation energy cost profile.

The cost of substation C^S is represented as an hourly curve in Fig. 2. The following marginal costs are assumed: for conventional generation C^C = €150/MWh [27]. For line losses, C^{LOSS} = €5/MWh; for wind generation, C^{RN} = €17/MWh [28]. For a generic storage model with a maximum capacity of 0.3 p.u. we have assumed a marginal cost C^{St} = €5-17/MWh [29]. In addition, in order to penalize the consequences of any unserved energy, we have assumed a maximum cost of C^{NS} = €200/MWh. The unserved energy, defined as a continuous variable, is the cost component of the objective function, considered for penalizing (assigning higher costs) unserved energy, where this variable should be minimized since its role is to raise the system cost in case the demand at a specific bus is unsatisfied.

B. Power demand profiles

The demand profile is obtained from the Iberian electricity market web site [30], in this case the power demand for the Canary islands on January 31, 2015, for a period of 24 hours.

This article has been accepted for publication in a future issue of this journal, but has not been fully edited. Content may change prior to final publication. Citation information: DOI 10.1109/TSTE.2016.2546279, IEEE Transactions on Sustainable Energy

In order to keep the scale factor and the demand profile, the latter is normalized dividing each nodal demand by the base load, this being 5 MW, a load that is slightly bigger than all the network loads considering the load variation for a period of 24 hours of operation. Hence, it represents the minimum (valley) and maximum (peak) loading limits. For the present case study, the maximum demand is located at node 61, where wind generation is also located.

C. Wind power scenarios

Concerning the hourly profile for renewable power generation, there are several ways of generating hourly wind power data in a synthetic way in literature. Nevertheless, the present model uses synthetically-generated stochastic wind scenarios which consider the autocorrelation that exists between consecutive observations of the wind power time series, the hourly profile of the expected wind power production and its corresponding forecasting error, as proposed by [31].

The initial profile is obtained from the Spanish market operator's website [32], for the wind power generation for 24 hours, as illustrated in Fig. 3. This reference data is used as an average forecast value for wind generation assuming a standard deviation of 15%. The scenario generation process consists of producing several randomly-generated sets of scenarios, using a first-order AR Markov process. Then, generation data are obtained using a probability transformation process similar to the one used in HOMER [33] to generate a synthetic wind generation profile. Some scenarios with extreme and unlikely values are excluded from the set of scenarios according to the magnitude of the forecasting error, if they are within the confidence intervals in all hours. After this filtering is performed, for the remaining sets, the scenarios are selected applying the K-means clustering algorithm. This way a combination of correlated behaviors and hourly profiles of wind generation scenarios provides the expected wind power production. A detailed explanation of the specific details for the generation of synthetic wind scenarios can be found in [31].

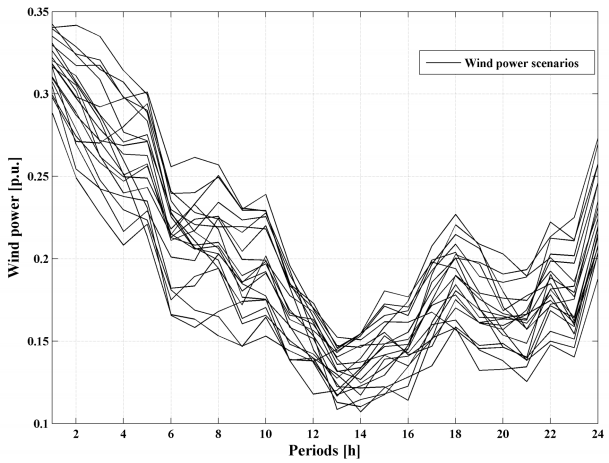

Fig. 3. Wind power scenarios.

Consequently, the scenarios shown above are selected according to the estimated forecasting error, giving a more consistent set of generation scenarios. The renewable generation model comprises 20 wind scenarios with hourly generation. The model is programmed in GAMS [34] using CPLEX solver in a computer with a Xeon E5-2687W processor at 3.1 GHz and 256 GB of RAM.

V. Results

The stochastic mixed linear programming (SMILP) presented has two stages; solved at the same time, as shown in equation (1). The stochasticity of wind generation is considered by means of 20 scenarios, where each of them has an equal probability of occurrence. For the resolution of the problem, a stochastic programming was chosen, where we can consider the uncertainties of the wind power generation to find an optimal solution considering all feasible options. Meanwhile, the deterministic option requires defined parameters and cannot deal with uncertainties. In this section, the results for the optimum reconfiguration and economic dispatch are presented for a daily configuration and for an hourly reconfiguration, where the impact of grid reconfiguration, wind participation and storage relocation on grid parameters is evaluated. Grid reconfiguration is performed using a mathematical formulation with appropriate constraints to guarantee the optimal radial configuration of the EDS. Also, the distribution grid has a set of ten switches, four tie switches (16-47, 28-66, 51-60, and 65-66) and the rest are sectionalizing switches (12-44, 13-14, 14-22, 15-16, 56-57, 62-63). The result shows that, out of ten switches, a maximum of five switches are necessary to guarantee grid radiality. Hence, according to the specific case of storage relocation, the following switches remain open as seen in Table I.

TABLE I
Hourly and daily reconfiguration

	Hourly reconfiguration		Daily reconfiguration	
Switches open	Sectionalizing	Tie	Sectionalizing	Tie
Storage location at bus 25	15-16, 56-57, 65-66	14-22, 12-44	13-14, 51-60, 62-63	14-22, 12-44
Storage location at bus 33	15-16, 56-57, 65-66	14-22, 12-44	15-16, 56-57, 28-66	14-22, 12-44

In Fig. 4 a voltage profile comparison is made for the base case scenario versus the daily single configuration and the hourly reconfiguration for the average wind power scenarios. The further we move from the substation to the last bus, the higher the voltage volatility. It is important to note that the incorporation of renewable generation at bus 61 and storage at bus 33 reduces voltage volatility considerably, while conventional generation at bus 25 is not accountable for that.

In addition, a comparison of the average voltage profiles for different reconfigurations versus the base case shows a tangible voltage profile improvement, which is more remarkable at buses 5-30 and buses 50-68. Specifically, the improvement in voltage profiles takes place at locations where there is storage and wind power injection, whereas the effect of such improvement in voltage profiles vanishes across the buses, far from these improvement points (buses). Comparing the impacts of reconfiguration on the voltage profiles for the daily reconfiguration versus the hourly reconfiguration, the hourly reconfiguration enhances the voltage profile significantly, especially where DG and storage are located, as shown in Fig.

This article has been accepted for publication in a future issue of this journal, but has not been fully edited. Content may change prior to final publication. Citation information: DOI 10.1109/TSTE.2016.2546279, IEEE Transactions on Sustainable Energy

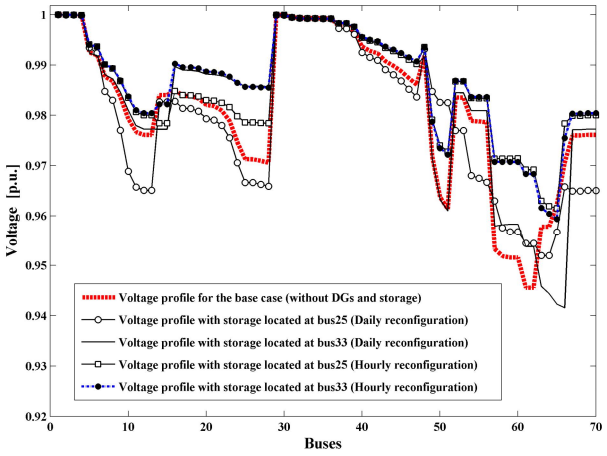

Fig. 4. Voltage profiles for the base case and different storage locations.

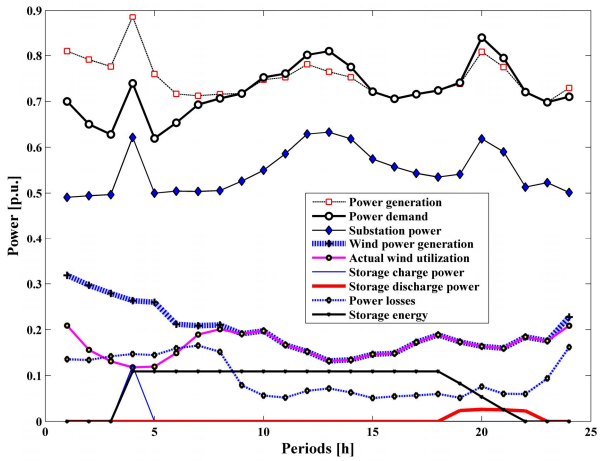

Fig. 5. Power profile for daily reconfiguration and storage at bus 33.

4. This is due to the fact that the grid is reconfigured (adapted) hourly to absorb the maximum possible wind generation. Even though this operation mode might be difficult to implement, this could be a snapshot of how future smart grid capabilities would look like.

Meanwhile, for the storage location at bus 33 (closer to the substation, as shown in Fig. 1), the hourly reconfiguration in Fig. 4 as well as the daily reconfiguration provide better voltage profiles compared to the storage location at bus 25 (in the middle of the network), as shown in Fig. 1). Such voltage profile improvement is true, with the exception of buses far from each storage location.

In Fig. 5, the power profile for the daily network reconfiguration (fixed configuration) with storage location at bus 33 is presented for a storage cost of €17/MWh. In this case, a greater portion of the power demand is satisfied but there is still unserved energy at both peak hours (in periods 12-17 and 21-23) This means that a significant amount of wind power is spilled (difference between wind power generation and actual wind utilization) at the beginning (in periods 1-8), which could be stored. However, the amount of energy stored is limited to 0.1 p.u. despite storage charging taking place at the beginning of the period in a peak wind period and storage discharging in a peak demand period.

In this case, when the storage is located at bus 33 (far from the wind generation), it is observed that the storage charging rate is low, due to the losses related to its distance from DG sources. However, this storage location helps to reduce the voltage drops in the main branch connected to the substation. In other words, the location of the storage at bus 33 enhances the voltage profile, but yields a lower storage capacity utilization. In contrast, if the storage is placed in the middle of the grid (at bus 25), as shown in Fig. 6., in addition to be closer to the wind generation, the storage is more charged compared to the location at bus 33. This is possible due to the fact that the storage at bus 25 is supplied by the injections from all sources at the expense of having voltage drops upstream, downstream and at the main branch, causing a lower voltage profile. In spite of this fact, the location at bus 25 provides a better storage capacity utilization for all the reconfiguration options.

In the aforementioned case, it is proved that storage charges partially, even for a storage cost as low as €5/MWh, since grid reconfiguration is not taking place to absorb the maximum wind power. Nevertheless, the amount of energy stored for a lower cost is bigger compared to the high cost case. In the case, when storage is located at bus 25, it is able to capture a significant amount of energy, as shown in Fig. 6 compared to the storage location at bus 33. This is due to lower resistive losses, given its proximity to wind generation. In addition, the energy stored and the discharge process are progressive (periods 1-21) as shown in Fig. 6.

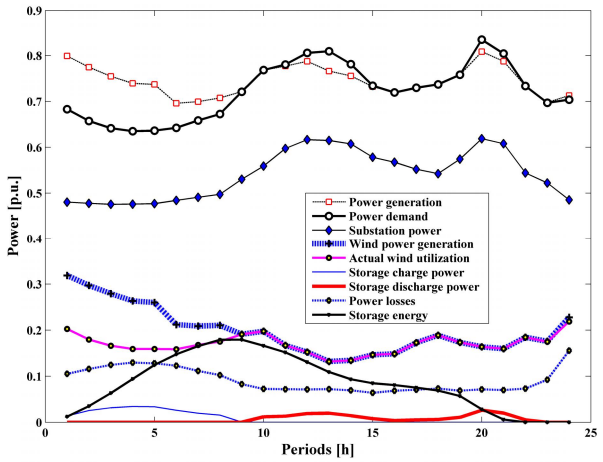

Fig. 6. Power profile for daily reconfiguration and storage at bus 25.

This can also be noted comparing the substation power participation. The difference between wind power generation and the actual wind utilization (spillage) for the storage location at bus 25 is less in comparison to the storage location at bus 33. This is due to the fact that storage at this location acts as an additional power support to the downstream buses. It can be noted that the storage location at bus 33 has disadvantages, mainly because the storage is not able to store the maximum

This article has been accepted for publication in a future issue of this journal, but has not been fully edited. Content may change prior to final publication. Citation information: DOI 10.1109/TSTE.2016.2546279, IEEE Transactions on Sustainable Energy

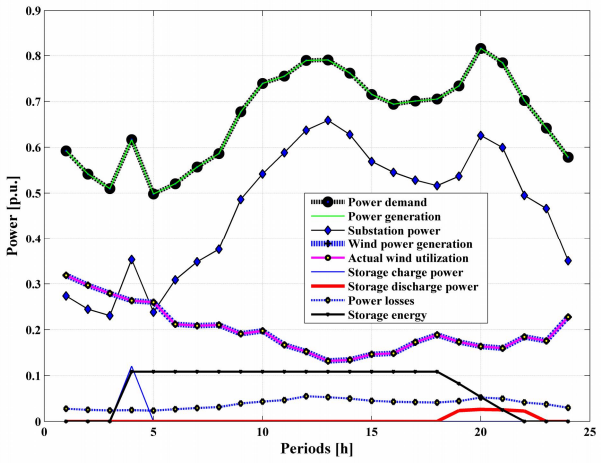

Fig. 7. Power profile for hourly reconfiguration and storage at bus 33.

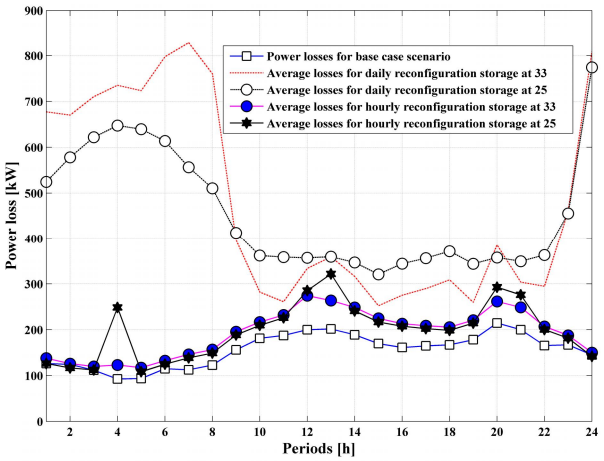

Fig. 9. Power losses for the base case and storage at buses 25 and 33.

possible wind power due to the longer distance from bus 61 (wind location) to bus 33 (storage location), constrained by higher resistive power losses. As a result, the amount of energy stored is reduced by half, compared to the storage location at bus 25, as illustrated in Fig. 6.

The power profile for the hourly reconfiguration is illustrated in Fig. 7 for the storage location at bus 33 and the power profile for the storage location at bus 25, as illustrated in Fig. 8. Unlike the case of daily reconfiguration, the grid is reconfigured each period in order to fully utilize wind generation. Therefore, the participation of the substation is significantly reduced at the beginning of the period, where wind generation is directly used to satisfy the demand. In both cases, a storage cost of €17/MWh has been assumed for charge and discharge. As a result, it can be noted that the substation power contribution in the first section (periods 1-8) is lower, while the contribution of wind is the maximum possible, as presented in Fig. 7.

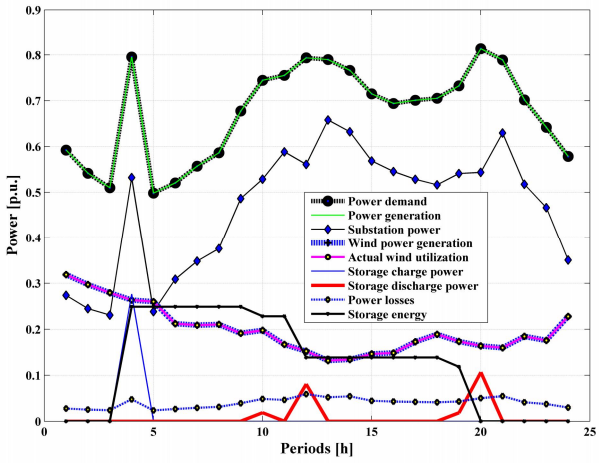

Fig. 8. Power profile for hourly reconfiguration and storage at bus 25.

In addition, for the case of storage located at bus 33, the energy storage is not significant compared to the storage capacity (0.3 p.u.). In contrast to the storage location at bus 25, the energy stored is comparable to the storage capacity (0.3 p.u.) in the first period, as shown in Fig. 8. Similar to the aforementioned case, wind generation is used to satisfy the demand, so that the power supply of the substation is reduced in comparison to the daily reconfiguration.

In all cases the storage located at bus 33, which is closer to the substation, behaves as a high demand bus: whenever the cost of electricity is lower the storage is charged, but not at full capacity, due to higher line resistive losses. On the contrary, the storage located at bus 25 (in the midstream of the network) is charged to its maximum value, allowing for a higher storage capacity and a better energy utilization.

Fig. 9 shows the power losses for the base case, daily and hourly reconfigurations, as well as the impact of swapping the storage locations from bus 25 to bus 33. Note that, when the wind power is minimum in the periods between hours 10-22, the power loss for the base case and for the rest of the cases is comparable (between 200-400 kW). On the other hand, the impact of the storage location on the amount of losses is minimal, in comparison to the impacts produced by the reconfigurations.

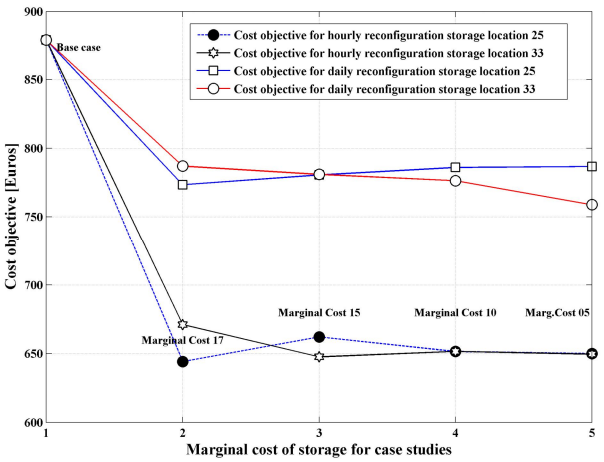

Fig. 10. Sensitivity analysis of storage location for changes in costs.

This means that, for hourly reconfigurations (for storage locations at buses 25 and 33), the difference in losses between them is minimal, but they have similar losses compared to the base case. Meanwhile, for the daily reconfiguration case, the losses are almost doubled, even though the difference

for storage locations 25 and 33 is comparable, peak losses occurring for a higher wind participation and storage charging. This result is consistent with the drawbacks explained previously about losses with the storage located at bus 33, with the exception of the charging and discharging periods. A sensitivity analysis is presented in Fig. 10 for the expected cost versus storage locations at buses 33 and 25, using daily and hourly network reconfigurations with variable storage costs. In this figure it can be seen that the expected cost improves for the daily and hourly network reconfigurations compared to the base case scenarios, especially for a storage cost lower than €17/MWh. The sensitivity analysis considering different storage marginal costs shows that a further decrease in the storage marginal cost to less than Euro 17/MWh does not necessarily guarantee a significant reduction in the expected cost objective. Comparing the reductions of the expected costs, the hourly configuration yields a better cost reduction. In relation to the impact of the storage location on cost reduction, no major expected cost reduction is achieved through swapping storage locations 25 and 33.

VI. Conclusions

This paper presented a 70-bus EDS on operation of wind and storage short-term impact analysis, using stochastic mixed integer linear programming. The new proposed SMILP model considered a single substation, wind generation, conventional generation and generic storage, with daily and hourly configurations, where the radiality of the EDS was guaranteed. As a result of network reconfiguration the voltage volatility for each bus was reduced incorporating wind generation and storage at specific buses. In addition, an analysis of their impacts on EDS performance was performed observing a reduction of the expected costs as well as the resistive losses. The participation of wind and storage, in spite of their substantial contribution on the improvement of the voltage profile, had a significant impact on the amount of resistive losses and expected system costs. Eventually, a sensitivity analysis on the impact of the location of storage on the expected costs was conducted. There was a meaningful reduction in the expected costs of EDS operation supported by DG in coordination with the substation. On top of that, the expected costs of the system were significantly reduced due to a higher participation of wind power. Broader analysis, considering multiple generation and storage even enforcing negative impacts on the system, would produce dramatic changes in the results and that would be interesting as a future research topic.

References

[1] H. E. Farag, E. El-Saadany, R. E. Shatshat, and A. Zidan, "A generalized power flow analysis for distribution systems with high penetration of distributed generation," *Electric Power Systems Research*, vol. 81, no. 7, pp. 1499–1506, April 2011.

[2] M. Grond, J. Morren, and J. Slootweg, "Integrating smart grid solutions into distribution network planning," in *IEEE PowerTech, Grenoble*, June 2013, pp. 1–6.

[3] A. Imran and M. Kowsalya, "Optimal distributed generation and capacitor placement in power distribution networks for power loss minimization," in *International Conference on Advances in Electrical Engineering (ICAEE)*, Jan 2014, pp. 1–6.

[4] A. Borghetti, "A mixed-integer linear programming approach for the computation of the minimum-losses radial configuration of electrical distribution networks," *IEEE Transactions on Power Systems*, vol. 27, no. 3, pp. 1264–1273, 2012.

[5] P. Meibom, R. Barth, B. Hasche, H. Brand, C. Weber, and M. O'Malley, "Stochastic optimization model to study the operational impacts of high wind penetrations in Ireland," *IEEE Transactions on Power Systems*, vol. 26, no. 3, pp. 1367–1379, 2011.

[6] F. Bouffard and F. Galiana, "Stochastic security for operations planning with significant wind power generation," *IEEE Transactions on Power Systems*, vol. 23, no. 2, pp. 306–316, May 2008.

[7] V. Farahani, B. Vahidi, and H. Abyaneh, "Reconfiguration and capacitor placement simultaneously for energy loss reduction based on an improved reconfiguration method," *IEEE Transactions on Power Systems*, vol. 27, no. 2, pp. 587–595, May 2012.

[8] T. Khalil, A. Gorpinich, and G. Elbanna, "Combination of capacitor placement and reconfiguration for loss reduction in distribution systems using selective pso," in *22nd International Conference and Exhibition on Electricity Distribution (CIRED 2013)*, June 2013, pp. 1–4.

[9] R. Gallano and A. Nerves, "Multi-objective optimization of distribution network reconfiguration with capacitor and distributed generator placement," in *IEEE Region 10 Conference TENCON 2014*, Oct 2014, pp. 1–6.

[10] L. Yang, M. He, V. Vittal, and J. Zhang, "Stochastic optimization based economic dispatch and interruptible load management with distributional forecast of wind farm generation," in *IEEE 53rd Annual Conference on Decision and Control (CDC), 2014*, Dec 2014, pp. 199–204.

[11] A. Arabali, M. Ghofrani, and M. Etezadi-Amoli, "Cost analysis of a power system using probabilistic optimal power flow with energy storage integration and wind generation," *International Journal of Electrical Power and Energy Systems*, vol. 53, pp. 832–841, 2013.

[12] H. Daneshi and A. Srivastava, "Impact of battery energy storage on power system with high wind penetration," in *IEEE PES Transmission and Distribution Conference and Exposition*, May 2012, pp. 1–8.

[13] M. Ghofrani and A. Arabali, "A stochastic framework for power system operation with wind generation and energy storage integration," in *IEEE PES Innovative Smart Grid Technologies Conference (ISGT)*, Feb 2014, pp. 1–5.

[14] R. Ferreira, C. Borges, and M. Pereira, "A flexible mixed-integer linear programming approach to the AC optimal power flow in distribution systems," *IEEE Transactions on Power Systems*, vol. 29, no. 5, pp. 2447–2459, Sept 2014.

[15] A. C. Rueda-Medina, J. F. Franco, M. J. Rider, A. Padilha-Feltrin, and R. Romero, "A mixed-integer linear programming approach for optimal type, size and allocation of distributed generation in radial distribution systems," *Electric Power Systems Research*, vol. 97, pp. 133–143, 2013.

[16] A. Zidan and E. F. El-Saadany, "Distribution system reconfiguration for energy loss reduction considering the variability of load and local renewable generation," *Energy*, vol. 59, pp. 698–707, 2013.

[17] R. Jabr, R. Singh, and B. Pal, "Minimum loss network reconfiguration using mixed-integer convex programming," *IEEE Transactions on Power Systems*, vol. 27, no. 2, pp. 1106–1115, 2012.

[18] A. Zidan and E. F. El-Saadany, "Incorporating load variation and variable wind generation in service restoration plans for distribution systems," *Energy*, vol. 57, pp. 682–691, 2013.

[19] J. F. Franco, M. J. Rider, M. Lavorato, and R. Romero, "A mixed-integer LP model for the reconfiguration of radial electric distribution systems considering distributed generation," *Electric Power Systems Research*, vol. 97, pp. 51–60, 2013.

[20] L. Tang, F. Yang, and J. Ma, "A survey on distribution system feeder reconfiguration: Objectives and solutions," in *IEEE PES Innovative Smart Grid Technologies-Asia*, 2014, pp. 62–67.

[21] S. H. Mirhoseini, S. M. Hosseini, M. Ghanbari, and M. Ahmadi, "A new improved adaptive imperialist competitive algorithm to solve the reconfiguration problem of distribution systems for loss reduction and voltage profile improvement," *International Journal of Electrical Power & Energy Systems*, vol. 55, pp. 128–143, 2014.

[22] J. Mendoza, R. Lopez, D. Morales, E. Lopez, P. Dessante, and R. Moraga, "Minimal loss reconfiguration using genetic algorithms with restricted population and addressed operators: real application," *Power Systems, IEEE Transactions on*, vol. 21, no. 2, pp. 948–954, May 2006.

[23] M. Lavorato, J. F. Franco, M. J. Rider, and R. Romero, "Imposing radiality constraints in distribution system optimization problems," *IEEE Transactions on Power Systems*, vol. 27, no. 1, pp. 172–180, 2012.

[24] C. Lueken, P. Carvalho, and J. Apt, "Distribution grid reconfiguration reduces power losses and helps integrate renewables," *Energy Policy*, vol. 48, pp. 260–273, 2012.

This article has been accepted for publication in a future issue of this journal, but has not been fully edited. Content may change prior to final publication. Citation information: DOI 10.1109/TSTE.2016.2546279, IEEE Transactions on Sustainable Energy

[25] C. Abbey and G. Joos, "A stochastic optimization approach to rating of energy storage systems in wind-diesel isolated grids," *IEEE Transactions on Power Systems*, vol. 24, no. 1, pp. 418–426, 2009.
[26] D. Pozo, J. Contreras, and E. Sauma, "Unit commitment with ideal and generic energy storage units," *IEEE Transactions on Power Systems*, vol. 29, no. 6, pp. 2974–2984, 2014.
[27] LAZARD. (2014) Lazard lcoe analysis version 8.0. [Online]. Available: http://www.lazard.com.
[28] Spanish Renewable Energy Plan for 2005–2010. [Online]. Available: http://www.idae.es/uploads/documentos/documentos_PER_2005-2010_8_de_gosto-2005_Completo.(modificacionpag_63)_Copia_2_301254a0.pdf.
[29] PNNL. (2013) national assessment of energy storage for grid balancing and arbitrage, phase II. volume 2: Cost and performance characterization. [Online]. Available: http://energyenvironment.pnnl.gov/pdf/National_Assessment_Storage_PHASE_II_vol_2_final.pdf.
[30] REE. (2015) Canary electricity demand in real-time. [Online]: http://www.ree.es/en/activities/canary-islands-electricity-system/canary-electricity-demand-in-real-time.
[31] G. Osório, J. M. Lujano-Rojas, J. C. O. Matias, and J. P. S. Catalão, "A fast method for the unit scheduling problem with significant renewable power generation," *Energy Conversion and Management*, vol. 94, pp. 178–189, 2015.
[32] REE. (2015) ESIOS generation and consumption. [Online]. Available: http://www.esios.ree.es/en/analysis/541.
[33] (2016) HOMER. the hybrid optimization model for electric renewables). [Online]: http://www.homerenergy.com.
[34] A. Brooke, D. Kendrick, A. Meeraus, and R. Raman, "GAMS/CPLEX: A Users Guide," *GAMS Development Corporation (2003)*, 2003.

Abebe W. Bizuayehu (M'15) received the M.Sc. degree in mechanical engineering, in the specialty of industrial mechanics from José Antonio Echevarría Higher Polytechnic Institute (I.S.P.J.A.E), Havana, Cuba, in 1989, and the Ph.D. degree in Renewable Energy and Energetic Efficiency from the University of Zaragoza, Spain, in 2012. He is currently a Post-doctoral fellow in UBI and INESC-ID and Researcher in European project "SiNGULAR", FP7, in University of Beira Interior, Portugal

Agustín A. Sánchez de la Nieta (M'15) received the B.S. and Ph.D. degrees in industrial engineering from the University of CastillaLa Mancha, Ciudad Real, Spain, in 2008 and 2013, respectively.

He is currently a Post-doctoral fellow in UBI and INESC-ID and Researcher in European project "SiNGULAR", FP7, in University of Beira Interior, Portugal. His research interests include power systems planning and economics, electricity markets, forecasting, and risk management for renewable energy sources.

Javier Contreras (SM'05-F'15) received the B.S. degree in Electrical Engineering from the University of Zaragoza, Zaragoza, Spain, in 1989, the M.Sc. degree from the University of Southern California, Los Angeles, in 1992, and the Ph.D. degree from the University of California, Berkeley, in 1997.

He is currently Full Professor at the University of Castilla-La Mancha, Ciudad Real, Spain. His research interests include power systems planning, operations and economics, and electricity markets.

João P. S. Catalão (M'04-SM'12) received the M.Sc. degree from the Instituto Superior Técnico (IST), Lisbon, Portugal, in 2003, and the Ph.D. degree and Habilitation for Full Professor ("Agregaão") from the University of Beira Interior (UBI), Covilhã, Portugal, in 2007 and 2013, respectively.

Currently, he is a Professor at the Faculty of Engineering of the University of Porto (FEUP), Porto, Portugal, and Researcher at INESC-ID - Lisbon and C-MAST/UBI. He has been the Primary Coordinator of the EU-funded FP7 project SiNGULAR ("Smart and Sustainable Insular Electricity Grids Under Large-Scale Renewable Integration"), a 5.2 million euro project involving 11 industry partners. He has authored or coauthored more than 400 publications, including, among others, 131 journal papers, 249 conference proceedings papers and 20 book chapters, with an h-index of 25 (according to Google Scholar), having supervised more than 30 post-docs, Ph.D. and M.Sc. students. He is the Editor of the books entitled Electric Power Systems: Advanced Forecasting Techniques and Optimal Generation Scheduling (Boca Raton, FL, USA: CRC Press, 2012) and Smart and Sustainable Power Systems: Operations, Planning and Economics of Insular Electricity Grids (Boca Raton, FL, USA: CRC Press, 2015). His research interests include power system operations and planning, hydro and thermal scheduling, wind and price forecasting, distributed renewable generation, demand response and smart grids.

Prof. Catalão is an Editor of the IEEE TRANSACTIONS ON SMART GRID, an Editor of the IEEE TRANSACTIONS ON SUSTAINABLE ENERGY, and an Associate Editor of the IET Renewable Power Generation. He was the Guest Editor-in-Chief for the Special Section on "Real-Time Demand Response" of the IEEE TRANSACTIONS ON SMART GRID, published in December 2012, and he is currently the Guest Editor-in-Chief for the Special Section on "Reserve and Flexibility for Handling Variability and Uncertainty of Renewable Generation" of the IEEE TRANSACTIONS ON SUSTAINABLE ENERGY. He is the recipient of the 2011 Scientific Merit Award UBI-FE/Santander Universities and the 2012 Scientific Award UTL/Santander Totta. Also, he has won 4 Best Paper Awards at IEEE Conferences.